Talanta 92 (2012) 72–77

Contents lists available at SciVerse ScienceDirect

Talanta

journal homepage: www.elsevier.com/locate/talanta

Multiplexed detection of tumor markers with multicolor quantum dots based on fluorescence polarization immunoassay

Jianniao Tian*, Liujin Zhou, Yanchun Zhao, Yuan Wang, Yan Peng, Shulin Zhao

Key Laboratory for the Chemistry and Molecular Engineering of Medicinal Resources (Ministry of Education of China), College of Chemistry and Chemical Engineering of Guangxi Normal University, Guilin 541004, China

ARTICLE INFO

Article history:
Received 20 October 2011
Received in revised form 21 January 2012
Accepted 29 January 2012
Available online 2 February 2012

Keywords:
Multiplexed detection
Fluorescence polarization Immunoassay
Tumor markers

ABSTRACT

A multicolor quantum dot (QD)-based nanosensor for multiplex detection of two tumor markers in a homogeneous format based on fluorescence polarization immunoassay was proposed. QDs520 and QDs620 were labeled alpha-fetoprotein(α-AFP) and carcinoembryonic antigen (CEA), respectively. After separated and purified by ultrafiltration, they were used in fluorescence polarization immunoassay for the simultaneous detection of human serum alpha-fetoprotein and carcinoembryonic antigen. Under the optimal conditions, the multi-analyte immunosensor had a wide linear range (from 0.5 ng mL^{-1} to 500 ng mL^{-1}) for both two tumor markers and good correlation (0.996 for α-AFP and 0.993 for CEA). The detection limits (LOD) were 0.36 ng mL^{-1} for CEA and 0.28 ng mL^{-1} for α-AFP (S/N = 3). The carcinoembryonic antigen and fetoprotein in clinical serum samples were simultaneously detected. The results from 28 serum samples had a good agreement with enzyme-linked immunosorbent assay (ELISA). The relative standard deviation and the recovery suggested that the precision and the accuracy of this analytical method were satisfactory. This strategy with high sensitivity, good specificity, easy procedures and short analysis time shows great promise for clinical diagnoses and basic discovery. The application of QDs with longer fluorescence lifetime and small fluorescence polarization can be used for the determination of high molecular-weight substances which cannot be analyzed using dye fluorescence polarization immunoassay.

1. Introduction

Recently, immunosensors and immunoassay methods for single-tumor markers have been well developed for cancer screening [1–3]. Their applications are facing great challenges, because most markers are not specific to a particular tumor, no single marker can be used for accurately predicting disease in all stages of infection. Panels of tumor markers can improve their diagnostic value in complex biological samples [4]. Thus the development of highly sensitive and selective sensors capable of simultaneous detection of multiple analytes has attracted much attention in the scientific community [5]. Compared with the traditional single-analyte immunoassay, the simultaneous multiplexed immunoassay is more efficient in clinical application since it can quantitatively detect a panel of biomarkers in a single run with improved diagnostic specificity. Moreover, the multiplexed immunoassay can shorten analytical time, enhance detection throughput, and decrease sampling volume and detection costs [6,7]. Thus, it has been quickly developed using different measurement techniques. Indeed, recent works by several groups have been proposed to perform simultaneous multianalyte immunoassays, including electrochemistry [8], multichannel waveguides [9], plasma mass spectrometry [10], and protein chip [11]. Hu et al. [12] proposed a protein chip combined the high-throughput capabilities of a microfluidic network with the high sensitivity and multicolor imaging ability offered by highly fluorescent QDs, which would become a promising diagnostic tool in clinical applications. Ma et al. [13] prepared the multicolor QD-encoded fluorescent microspheres by deposition of different colors water soluble CdTe QDs through layer-by-layer self-assembly for the analysis of human IgG and rabbit IgG antigen. However, most of them are heterogeneous immunoassay, which need to separate the free form from the complex of the antigen and the antibody, so that accuracy and sensitivity of the assay are generally dependent on the quality of the separation, and easily affected by sample composition [14].

Fluorescence polarization (FP), because of its homogeneous format, speed, accuracy, and automated high-throughput capability,

Abbreviations: QD, quantum dot; α-AFP, alpha-fetoprotein; CEA, carcinoembryonic antigen; LOD, the detection limits; ELISA, enzymelinked immunosorbent assay; FPIA, fluorescence polarization immunoassay; EDC, 1-ethyl-3(3-dimethy laminopropyl) carbodiimide hydrochloride; NHS, N-hydroxysuccinimide; TGA, thioglycollic acid.

* Corresponding author. Tel.: +86 7735846279; fax: +86 7735832294.
E-mail address: tianjn58@yahoo.com.cn (J. Tian).

0039-9140/$ – see front matter © 2012 Elsevier B.V. All rights reserved.
doi:10.1016/j.talanta.2012.01.051

constitutes one of the most employed techniques for the routine analysis of small molecules in a variety of application fields including clinical, food, and environmental areas [15–17]. Fluorescence polarization immunoassay (FPIA) is based on the competition of free (unlabeled) analyte and fluorescent-labeled antigen for antibody binding sites. Fluorescence emission is detected after excitation of the fluorescent probes with the plane-polarized light. The fluorescence polarization value is indirectly proportional to the analyte concentration as the analyte can bind to the high molecular weight species-like antibody [18,19]. It does not require a separation step to isolate antibody-bound label from unbound immunoreagent and is almost unique in this regard in small molecule (hapten) immunoassays [20,21].

Semiconductor quantum dots (QDs) represent a revolution in the application of fluorophores in fluorescent labeling due to their high photo- and chemical stability and high quantum yield, as compared to traditional organic dyes [22,23]. In addition, different QD fluorescence emissions can be controlled by simply adjusting the QD size. Furthermore, all colors of QDs can be excited by a single excitation source, which makes it much easier to achieve multiplexed detection than traditional dyes that require the excitation light source be tuned into their respective narrow absorption bands [24,25].

Traditionally, the fluorescein, which has short fluorescence lifetime and great fluorescence polarization, was used as fluorescent probe in fl polarization immunoassay. Only the determination of low molecular-weight substances, such as therapeutic agents, drugs of abuse and hormones is considered because the measured change in fluorescence polarization depends on the molecular size of the analyte and the fluorescence polarization of fluorescein [26]. Sanchez-Martinez et al. used long-lived fluorophores such as Nile Blue and a ruthenium(II) chelate for the application in PFIA and PFIA development for macromolecular antigens [27,28]. QDs with longer fluorescence lifetime and small fluorescence polarization could be used for the determination of high molecular-weight substances, because the significant change in fluorescence polarization could be detected after attached to antigen. Previous work has been done in our laboratory to develop a fluorescence polarization immunoassay for detection of alpha-fetoprotein in human serum, indicating that QDs are attractive fluorescent probes in fluorescence polarization immunoassay [29]. In this article, we report on a portable multicolor quantum dot-based fluorescence polarization immunoassay (FPIA) for simple, sensitive, and selective detection of carcinoembryonic antigen (CEA) and α-fetoprotein (α-AFP) in human serum. The approach developed in this work combines the advantage of the FPIA and the high sensitivity and the stability of quantum dot resulting in a novel, portable, and rapid competitive immunoassay tool for sensitive and selective multiplexed detection of tumor markers.

2. Materials and methods

2.1. Reagents and instruments

1-Ethyl-3(3-dimethy laminopropyl) carbodiimide hydrochloride (EDC) and *N*-hydroxysuccinimide (NHS) were purchased from Sigma–Aldrich. We purchased carcinoembryonic antigen (CEA), α-fetoprotein (α-AFP), CEA and α-AFP monoclonal antibodies from Shuangliu Zhenglong Laboratory of Biochemical Products (Chengdu, China). The concentrations of CEA, α-AFP, anti-CEA and anti-α-AFP stock solutions were 1.5 g/L, 1 g/L, 2.5 g/L and 2.3 g/L, respectively. All other reagents were of analytical reagent grade and used without further purification. We prepared 0.02 mol/L PBS of various pH values by mixing the stock solutions of NaH_2PO_4 and Na_2HPO_4 and adjusting the pH with 0.02 mol/L NaOH and H_3PO_4. We used purified water (18 MΩ/cm) for all experiments.

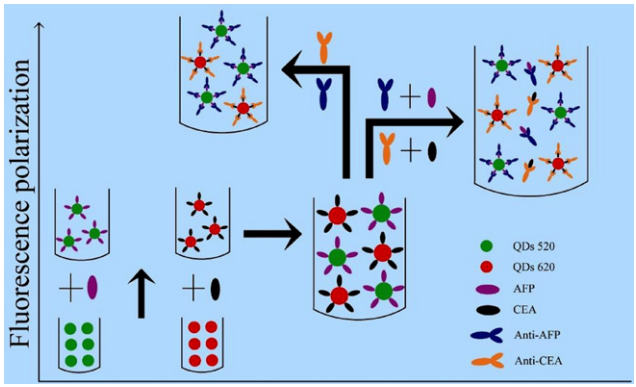

Fig. 1. Schematic diagram of the multicolor fluorescence polarization immunoassay procedure.

Photoluminescence (PL) measurements were performed at room temperature using a LS-55 luminescence spectrometer (Perkin Elmer, USA). The fluorescence polarization immunoassay was performed on an automated polarization model FL3-P-TCSPC (HORIBA JOBIN YVON, France).

2.2. Synthesis of CdTe/CdS QDs

Highly fluorescent CdTe QDs nanocrystals were synthesized by our laboratory according to a protocol adapted form [30]. Then the purify CdTe core QDs were injected into the Cd^{2+}–TGA (thioglycollic acid) precursor solution ($[Cd^{2+}]/[TGA] = 1$, pH = 9.0). The CdTe/CdS precursor solution was put into a flask, the solution was heated to 80 °C in argon atmosphere and the thioacetamide (TAA) solution was injected into the flask with continuous stirring. The CdTe/CdS core–shell QDs (PLQY ≈ 60%, determined by comparative method [31]) were obtained after different refluxing times. All of the nanocrystals were purified by acetone precipitation and then dissolved in PBS. The stock solutions of multicolor CdTe/CdS QDs were both 1.25×10^{-3} mol/L.

2.3. Antigen labeling

The α-AFP and CEA were labeled with QDs520 and QDs620 respectively. Briefly, 1 mg/L antigen in 50 mmol/L Tris–HCl buffer (pH 6.8) was added into 0.125 mmol of QDs followed by the addition of 100 μL 20 mg/mL EDC and 100 μL 10 mg/mL NHS and incubated at 4 °C overnight. The free non-conjugated QDs were removed by ultrafiltration using a 50,000 MW filter.

2.4. Assay protocol

Fig. 1 shows the schematic diagram of the fluorescence polarization immunoassay procedure. Specific steps as follows: 700 μL of antigen standard solutions mixture, 700 μL of purify antigen-QDs solution mixture and 700 μL of the optimal dilution of antibody mixture were added into a cuvette. The reaction mixture was vortex-mixed, allowed to stand for 15 min, and then the fluorescence polarization values were measured in the fluorescence spectrophotometer. Serum samples were carried out on a 10,000 MW size filter and centrifugation at 3000 × *g* for 15 min at 4 °C to remove low molecular weight protein (<10,000 Da). The upper phase was decanted, dissolved in PBS and carried out on a 200,000 MW size filter again and centrifugation at 3000 × *g* for 15 min at 4 °C to remove high molecular weight protein

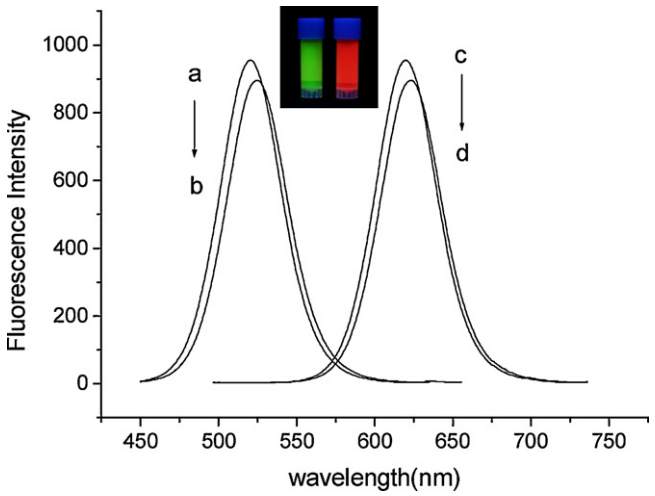

Fig. 2. Fluorescence emission spectra of QDs520 and QDs620: (a) QDs520, (b) α-AFP–QDs520, (c) QDs620 and (d) CEA–QDs620. Excitation wavelength is 370 nm and the concentration of QDs nanocrystal is 3×10^{-4} mol/L. 0.02 mol/L PBS (pH 6.8); 25 °C.

(>200,000 Da), the lower sample was dissolved with PBS buffer for CEA and the AFP analysis.

All experiments were carried out at 25 °C. The fluorescence intensity and fluorescence polarization of the immunocomplex were monitored by exciting the sample at 370 nm and measuring the emission at 520 nm and 620 nm. Fluorescence polarization was measured using the L-format configuration, using FluorEssence™ software such as constant wavelength analysis to achieve a polarization value. The polarization value was also calculated automatically by the instrument. The integration time was set to 3 s for the polarization measurements. Over ten polarization measurements were taken each time, and they were then averaged for further data processing. The relative standard deviation was 2% for all measurements.

2.5. Sample collection

Blood samples were collected from 28 patients at the First People Hospital of Nanning (Guangxi, China), after the patients gave informed consent. After clotting, the serum and packed cells were separated by centrifugation at $1000 \times g$. The serum samples were then stored at −20 °C under nitrogen gas until they were assayed.

3. Results and discussion

3.1. Characterization of antigen-QDs

Accounting the sensitivity and the specificity of immunoassay, QDs520 and QDs620 were used as fluorescence sensors, because of their narrow emission bandwidths in the same excitation wavelength. As shown in Fig. 2a, when they were both excited 370 nm, their emission peaks separated completely, which demonstrated that the interaction of their fluorescence polarization values can be ignored.

Activated by EDC and NHS mixture, CEA and AFP were linked to QDs via the chelating of carboxylic groups on QDs with amino groups of antigen. As shown in Fig. 2a, the results shown that their spectra were very similar with the same luminescence efficiency and spectral width. However a red shift about 5 nm of the luminescence peak of CEA-QDs or α-AFP-QDs was observed as compared with that of un-conjugated QDs. Such a small spectral shift of the luminescence peak seems the characteristic of the ligand absorption on the QD surface [32]. It has been reported recently that the decylamine conjugation to CdSe QDs as well as the addition of mercaptan to the amine-capped CdSe surfaces all caused a luminescence spectral red-shift of about 4 nm due to the electronic effects of the ligand [33]. It is also shown in Fig. 2a that the fluorescence intensity of antigen-QDs was lower than that of QDs alone (for the same total concentration of QDs). This phenomenon probably was due to electron transfer mechanism on the surface of QDs. The rearranged gross electrostatic/polar environment of inorganic core and its attendant effects on the efficiency of excitation likely led to the observed quenching in the fluorescence intensity [34].

3.2. Optimization of immunoreaction

The QDs solution of different pH values was used for conjugation of antigen. The mixtures were vigorously stirred at room temperature for 15 min. Fig. 3a–c shows the fluorescence emission spectra of QDs and QDs–antigen conjugate at different pH. It can be seen that the emission peak of the QDs–antigen conjugate all undergoes a slightly red shift at various pH (6.1, 6.8, 7.2, 7.5) and the fluorescence intensity of QDs–antigen all declined slightly, which reduced more significant in a partial alkaline environment (pH7.50), although compared with that in other acidity, the fluorescence intensity of QDs in the circumstances was stronger. Considering the fluorescence intensity of quantum dots in the acidic environment also declined, the PBS buffer of pH 6.8 was fit for this work. The effect of pH on the AFP–QDs520 was similar with CEA–QDs620 and data were not shown.

As reported, the lower QDs-labeled antigen concentration, which have no effect on the fluorescence signal, the lower sensitivity will be obtained. In previous studies, the lowest QDs-labeled antigen concentration is that its fluorescence signal should be approximately 10 times higher than the background signal from PBS (total fluorescence intensity) [18]. So, here, the amount of antigen–QDs was selected such that the total final fluorescence intensity was 10 times higher than the background of PBS.

The amount of antibodies in the incubation solution was a key in the competitive immunoassay format. The effects of dilutions of antibodies in the incubation solution on the fluorescence polarization were shown in Fig. 4a. The specific monoclonal antibodies gave significant binding with QDs-labeled antigen at higher concentration and slowly decreased in FP as antibodies became more diluted by PBS. The results indicated that the QDs-labeled antigen was successfully synthesized and could be used as a competition agent in the FPIA. Furthermore, an excellent immunosensor array must exclude cross-reactivity between analytes and nonconjugated antibodies [35]. Thus, the specific monoclonal anti-AFP was added to the AFP–QDs520 and CEA–QDs620 mixture, as shown in Fig. 4b, when anti-AFP was added the CEA–QDs620 always had similar FP values in spite of the change of nonspecific anti-AFP concentration, while the AFP–QDs520 showed the maximum responses on FP values due to the saturated binding at high concentrations, further dilutions resulted in the decrease of FP values of the AFP–QDs520. Thus the cross-reactivity and nonspecific binding were negligible, suggesting that the two tumor markers could be assayed individually in a single run without interference. As reported the dilution of antibody corresponding to 50% QDs-labeled antigen binding was chosen as the titer value because this dilution may be optimal for FPIA standard curves [36,37], which persisted to dilutions of 1:1500 for anti-AFP antibody, 1:1800 for anti-CEA antibody. Thus, the incubation solution was prepared according to the optimal dilutions.

3.3. The standard cure for tumor markers determination

As shown in Fig. 5 in the fixed concentration of antibody solution, labeled and unlabeled antigens were allowed to

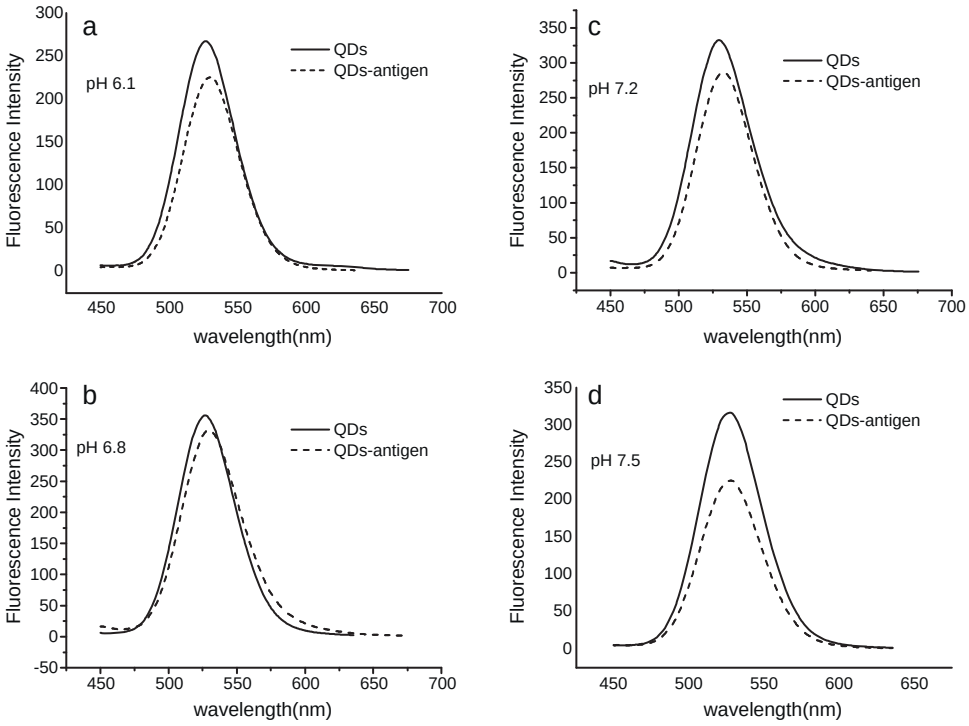

Fig. 3. Emission spectrum of the QDs and QDs–antigen solution at different pH values: (a) pH 6.1, (b) pH 6.8, (c) pH 7.2 and (d) pH 7.5. Excitation wavelength is 370 nm and the concentration of QDs nanocrystal is 3×10^{-4} mol/L. 0.02 mol/L PBS; 25 °C.

simultaneously compete for the binding sites on the antibody. The concentration of labeled antigen was fixed, and the concentration of unlabeled antigen was changed. When unlabeled antigen was added, the polarization signals were obviously weaken with the increase of its concentration. The analyte concentrations and the polarization signal were fitted to a sigmoid curve according to the formula: $Y = (A_1 - A_2)/[1 + (X/X_0)^p] + A_2$, where A_1 and A_2 are the maximal and minimal polarization signals, p is the slope of the sigmoid curve, and X_0 expressed as IC_{50} value [18]. The sigmoid curve fitting and calibration plots were all shown in Fig. 5. The inset plot in Fig. 5 was the calibration curve of AFP and CEA, it showed that it had good linear relation in the range of 0.5–500 ng mL^{-1} with $P = 119–24.3$ lgC (ng mL^{-1}) ($R^2 = 0.993$) for CEA and 0.5–500 ng mL^{-1} with $P = 147–33.5$ lgC (ng mL^{-1}) ($R^2 = 0.996$) for AFP, P was the polarization (mP) values and lgC was the logit value of antigen concentration. Each

Table 1
Results of the determination of AFP in serum samples ($n = 5$).

Sample number	Content (ng mL^{-1})	Increment (ng mL^{-1})	Total content (ng mL^{-1})	Recovery (%)	RSD (%)	ELISA (ng mL^{-1})
1	7.36	10	17.52	101.6	0.86	8.14
4	9.88	10	20.36	104.8	2.68	9.08
6	203	100	298	95.0	4.36	205
7	89.4	50	137.6	96.4	2.92	90.8
9	218	100	312	94.0	1.85	195
10	126	100	219	93.0	1.63	131
13	6.83	10	17.32	104.9	2.45	7.12
14	32.6	50	81.4	97.6	3.16	46.8
17	22.4	50	72.9	101.0	3.06	21.5
19	204	100	308	104.0	2.18	217

Table 2
Results of the determination of CEA in serum samples ($n = 5$).

Sample number	Content (ng mL^{-1})	Increment (ng mL^{-1})	Total content (ng mL^{-1})	Recovery (%)	RSD (%)	ELISA (ng mL^{-1})
1	2.16	5	7.52	107.2	1.18	2.35
4	1.65	5	6.83	103.6	2.09	1.88
6	167	100	264	97.0	1.83	165
7	53.8	50	102.9	98.2	2.64	52.5
9	98.2	100	197.3	99.1	4.16	103
10	23.8	50	74.6	101.6	3.07	22.7
13	4.98	5	10.35	107.4	2.28	5.12
14	22.3	50	71.8	99.0	1.36	20.8
17	23.7	50	74.36	101.3	4.01	24.5
19	12.6	10	23.28	106.8	2.06	14.2

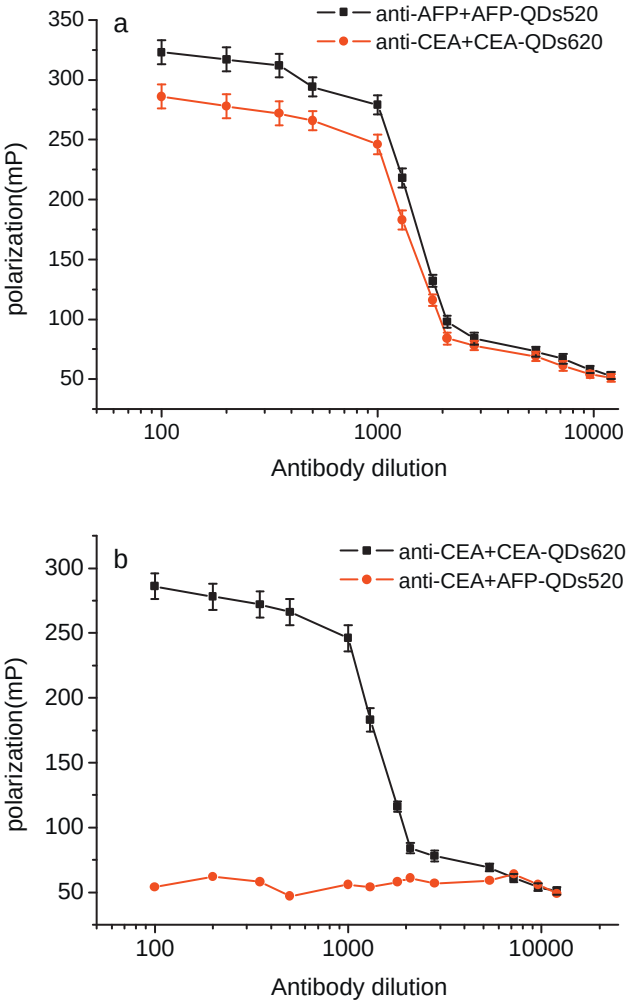

Fig. 4. Effects of working concentration of antibodies in incubation solution (a) on fluorescence polarization of the QDs–antigen array under other optimal conditions at room temperature, and control results of nonspecific (b). The original concentration of anti-CEA and anti-α-AFP diluted before was 2.5 and 2.3 μg/mL, respectively.

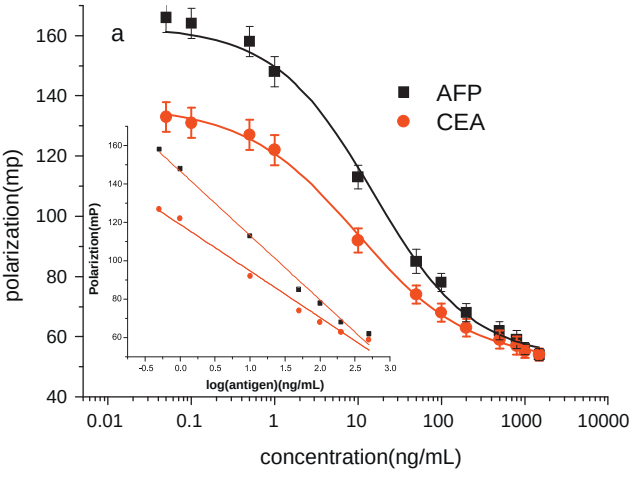

Fig. 5. FPIA calibration curves for two tumor markers: α-AFP (■); CEA (●). Inset: the linear range of CEA and α-AFP.

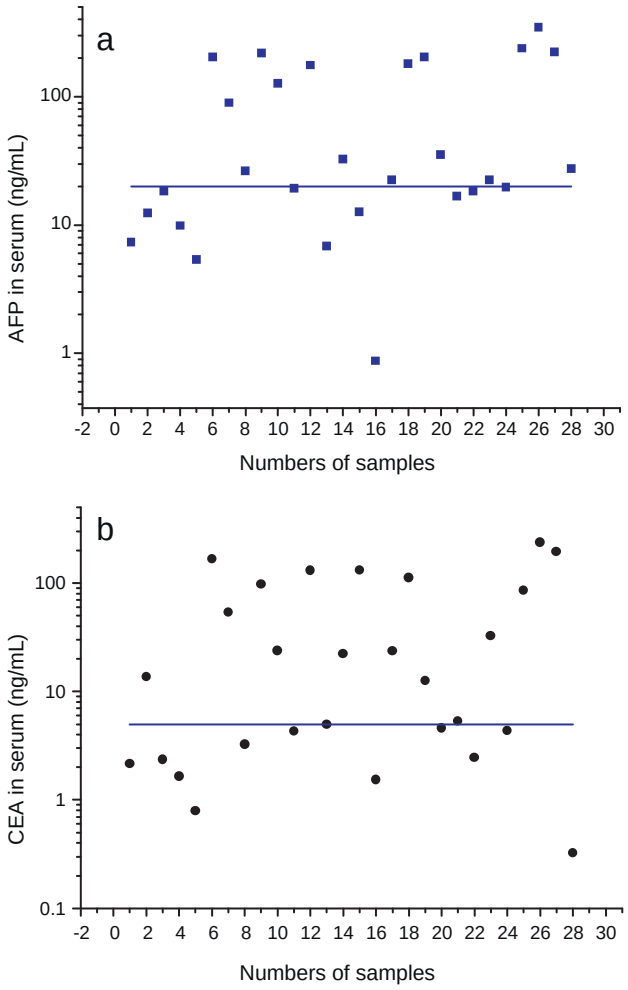

Fig. 6. Results of multianalyte simultaneous immunoassay of α-AFP (a), CEA (b) in human serum. α-AFP (■); CEA (●); threshold value (—).

measurement for date points was repeated about six times. The detection limits (LOD), which were determined from calibration curves using the blank signal [38], was 0.36 ng mL^{-1} for CEA and 0.28 ng mL^{-1} for α-AFP.

3.4. Application in simultaneous detection of serum multitumor markers

For analyses of practical samples, the interference and fluorescence quenching by some serum samples should be taken into account [29]. In this paper, the advanced process of centrifugation with an ultracentrifuge filter was performed to remove unrelated protein in the serum. After 700 μL serum sample was mixed with 700 μL mixture solution of purify QDs-labeled antigen with the optimized amount, 700 μL mixture solution of the optimal dilution of antibody were added into the resulting incubation. We simultaneously detected the concentrations of two tumor markers after the reaction mixture was vortex-mixed. The results of the simultaneous multianalyte detection with the proposed arrays for 28 serum samples are shown in Fig. 6, compared with those obtained using the commercial ELISA single-analyte testing [39,40]. For CEA the commercial ELISA assay showed that 13 of 28 samples were clinically negative and 15 samples were clinically positive (≥5 ng mL^{-1}), and our proposed method showed all CEA concentrations in these samples were in good agreement with these results, except the content of sample No. 21 was slightly higher than the threshold value, as shown in Fig. 6b, indicating acceptable reliability

for CEA. As shown in Fig. 6a, the results of α-AFP obtained with our proposed method showed that 9 of 28 samples were clinically negative and 19 samples were clinically positive ($\geq$20 ng mL^{-1}), which almost all were in good agreement with the commercial of testing.

In order to verify the stability and accuracy of our proposed method, the relative standard deviation (RSD) and the recovery of the fluorescence polarization immunoassay at different concentrations of the two tumor markers in ten serum samples was also listed in Tables 1 and 2. From Tables 1 and 2, the control results of ten samples indicated that the accuracy for α-AFP was acceptable, although sample No.14 and sample No. 19 were slightly higher or lower than the control value. The RSD were from 1.18% to 4.16% for CEA, 0.86% and 4.36% for α-AFP, indicating acceptable imprecision and fabrication reproducibility. The recoveries of CEA and α-AFP were 97.0%–107.4%, 93.0%–104%, respectively. Therefore, the fluorescence polarization immunoassay could be satisfactorily applied to the clinical diagnosis.

4. Conclusion

In conclusion, the proposed method showed excellent performance for simultaneous detection of CEA and α-AFP with wide linear ranges and low detection limits and acceptable stability, reproducibility, and accuracy. The convenient operation and ultrasensitivity of the proposed method provided a promising potential in clinical applications.

Acknowledgments

This work has been supported by National Natural Science Foundation of China (No. 21165004, 21163002), the Guangxi Natural Science Foundation of China (2010GXNSFF013001, 0728043), Innovation Plan in Graduate Education of Guangxi Province (2010106020703M70) and the project of Key Laboratory for the Chemistry and Molecular Engineering of Medicinal Resources (Guangxi Normal University), Ministry of Education of China (CMEMR2011-14).

References

[1] A.L. Ghindilis, P. Atanasov, M. Wilkins, E. Wilkins, Biosens. Bioelectron. 13 (1998) 113–131.
[2] J.H. Lin, H.X. Ju, Biosens. Bioelectron. 20 (2005) 1461–1470.
[3] Q.F. Li, D.P. Tang, J. Tang, B.L. Su, J.X. Huang, G.N. Chen, Talanta 84 (2) (2011) 538–546.
[4] J. Louhimo, P. Finne, H. Alfthan, U.H. Stenman, C. Haglund, Anticancer Res. 22 (2002) 1759–1764.
[5] C.Y. Zhang, J. Hu, Anal. Chem. 82 (2010) 1921–1927.
[6] N. Honda, U. Lindberg, P. Andersson, S. Hoffmann, H. Takei, Clin. Chem. 51 (10) (2005) 1955–1961.
[7] I. Nishizono, S. Lida, N. Suzuki, H. Kawada, H. Murakaml, Y. Ashihara, M. Okada, Clin. Chem. 37 (9) (1991) 1639–1644.
[8] J. Wu, F. Yan, J.H. Tang, C. Zhai, H.X. Ju, Clin. Chem. 53 (8) (2007) 1495–1502.
[9] H. Mukundan, H.Z. Xie, D. Price, J.Z. Kubicek-Sutherland, W.K. Grace, A.S. Anderson, J.S. Martinez, N. Hartman, B.I. Swanson, Anal. Chem. 82 (2010) 136–144.
[10] S.C. Zhang, C. Zhang, Z. Xing, X.R. Zhang, Clin. Chem. 50 (7) (2004) 1214–1221.
[11] M.S. Wilson, W.Y. Nie, Anal. Chem. 78 (2006) 6476–6483.
[12] M. Hu, J. Yan, Y. He, H.T. Lu, L.X. Weng, S.P. Song, C.H. Fan, L.H. Wang, ACS Nano 4 (1) (2010) 488–494.
[13] Q. Ma, X.Y. Wang, Y.B. Li, Y.H. Shi, X.G. Su, Talanta 72 (2007) 1446–1452.
[14] H.J. Yang, S.J. Jiang, Y.J. Yang, C.J. Hwang, Anal. Chim. Acta 312 (1995) 141–148.
[15] J.A. Cruz-Aguado, G. Penner, Anal. Chem. 80 (2008) 8853–8855.
[16] J. Ruta, S. Perrier, C. Ravelet, J. Fize, E. Peyrin, Anal. Chem. 81 (2009) 7468–7473.
[17] X.Q. Guo, F.N. Castellano, L. Li, J.R. Lakowicz, Anal. Chem. 70 (1998) 632–637.
[18] S.A. Eremin, N.R. Murtazina, D.N. Ermolenko, A.V. Zherdev, A.A. Mart'ianov, E.V. Yazynina, I.V. Michura, A.A. Formanovsky, B.B. Dzantiev, Anal. Lett. 38 (2005) 951–969.
[19] M.L. Steffes, G.W. Pittluck, M.E. Jolley, H.N. Panas, D.L. Olive, C.H.J. Wang, D.D. Nystrom, C.L. Keegan, T.P. Davis, S.D. Stroupe, Clin. Chem. 28 (11) (1982) 2278–2282.
[20] R.J. Straka, T.J. Hoon, R.L. Lalonde, J.A. Pieper, M.B. Bottorff, Clin. Chem. 33 (10) (1987) 1898–1900.
[21] N.R. Murtazina, S.A. Eremin, O.V. Mozoleva, S.J. Everest, A.J. Brown, R. Jackman, Int. J. Food Sci. Technol. 39 (2004) 879–889.
[22] C.S. Wu, M.K. Khaing Oo, X.D. Fan, ACS Nano 4 (10) (2010) 5897–5904.
[23] K.K. Jain, Clin. Chem. 53 (11) (2007) 2002–2009.
[24] J. Liu, S.K. Lau, V.A. Varma, B.A. Kairdolf, S.M. Nie, Anal. Chem. 82 (2010) 6237–6243.
[25] D.M. Willard, O.A. Van, Nat. Mater. 2 (2003) 575–576.
[26] M.C. Gutierrez, A. Gomez-Hens, D. Perez-Bendito, Talanta 36 (1989) 1187–1201.
[27] M.L. Sanchez-Martinez, M.P. Aguilar-Caballos, A. Gomez-Hens, Anal. Chem. 79 (19) (2007) 7424–7430.
[28] M.L. Sanchez-Martinez, M.P. Aguilar-Caballos, S.A. Eremin, A. Gomez-Hens, Talanta 72 (1) (2007) 243–248.
[29] J.N. Tian, R.J. Liu, Y.C. Zhao, Y. Peng, X. Hong, Q. Xu, S.L. Zhao, Nanotechnology 21 (2010) 305101–305108.
[30] J.N. Tian, R.J. Liu, Y.C. Zhao, Q. Xu, S.L. Zhao, J. Colloid Interface Sci. 336 (2009) 504–509.
[31] F.F. Suzanne, D. Lavabre, J. Chem. Educ. 76 (9) (1999) 1260–1264.
[32] F.L. Xue, J.Y. Chen, J. Guo, C.C. Wang, W.L. Yang, P.N. Wang, D.R. Lu, J. Fluoresc. 17 (2007) 149–154.
[33] C. Bullen, P. Mulvaney, Langmuir 22 (2006) 3007–3013.
[34] T. Takagahara, Phys. Rev. Lett. 71 (1993) 3577–3580.
[35] M.S. Wilson, W.Y. Nie, Anal. Chem. 78 (2006) 2507–2513.
[36] P. Onnerfjord, S. Eremin, J. Emneus, G. Marko-Varg, J. Immunol. Methods 213 (1998) 31–39.
[37] Z.H. Wang, L.L. Cheng, W.M. Shi, S.X. Zhang, J.Z. Shen, Sci. China Chem. 53 (3) (2010) 553–555.
[38] M. Pourfarzaneh, G.W. White, J. Landon, D.S. Smith, Clin. Chem. 26 (1980) 730–733.
[39] F. Niculescu, H.G. Rus, D. Ionescu, A. Maican, M. Petcovici, D. Malide, R. Rahaian, Arch. Roum. Pathol. Exp. Microbiol. 72 (1989) 47–52.
[40] A. Hullin, J.S. Woodhead, Clin. Chem. 31 (11) (1985) 1868–1870.